Chemical Synthesis

Mini Review

Research progress of photoelectrochemical conversion of CO_2 to C_{2+} products

Xia Jiang[1,2], Rui Chen[1,2], Yan-Xin Chen[1,2,3,*] (iD)**, Can-Zhong Lu[1,2,3,*]**

[1]State Key Laboratory of Structural Chemistry, Fujian Institute of Research on the Structure of Matter, Chinese Academy of Sciences, Fuzhou 350002, Fujian, China.
[2]Xiamen Key Laboratory of Rare Earth Photoelectric Functional Materials, Xiamen Institute of Rare-earth Materials, Haixi Institutes, Chinese Academy of Sciences, Xiamen 361021, Fujian, China.
[3]Fujian Science & Technology Innovation Laboratory for Optoelectronic Information of China, Fuzhou 350108, Fujian, China.

[*]**Correspondence to:** Prof. Yan-Xin Chen, Prof. Can-Zhong Lu, State Key Laboratory of Structural Chemistry, Fujian Institute of Research on the Structure of Matter, Chinese Academy of Sciences, 155 Yangqiao Road West, Fuzhou 350002, Fujian, China. E-mail: yanxinchen@fjirsm.ac.cn; czlu@fjirsm.ac.cn

Abstract

The reduction of CO_2 to C_{2+} products using photoelectrochemistry (PEC) is significant and highly challenging. However, systematic summaries on PEC CO_2 conversion into C_{2+} products are lacking. Therefore, this paper systematically reviews the current research status of the PEC CO_2 conversion for the preparation of C_{2+} products, including the pathways of C_{2+} products, the usage of catalysts and reactors, and methods for improving C_{2+} product selectivity. Besides, the deficiencies in current research are analyzed, and future developments are discussed.

Keywords: Photoelectrochemistry, C_{2+} products, CO_2 conversion

INTRODUCTION

The hazards of climate change to humans and the environment necessitate transitioning from our current fossil fuel economy to an economy based on renewable and carbon-neutral energy technologies. The urgency to reduce primary greenhouse gas (CO_2) emissions while continuing to provide fuel for the growing global population remains one of the most significant technological challenges of our time. Photoelectrochemical technology not only maximizes the advantages of photocatalysis and electrocatalysis,
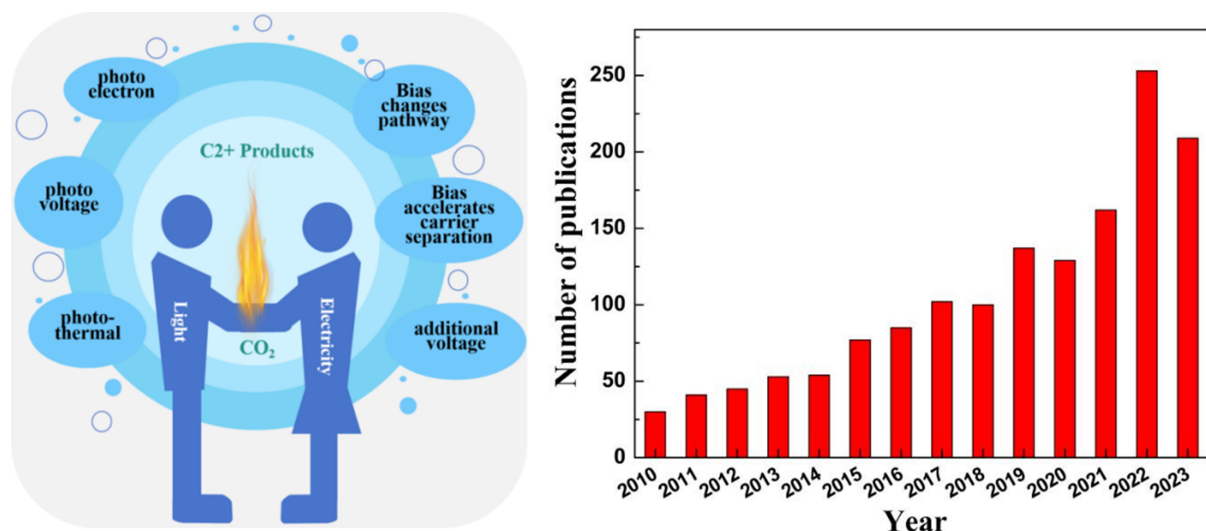
Figure 1. The role of light and electricity in photoelectrochemical CO_2 reduction and the number of publications on PEC CO_2 conversion were obtained using keyword search (photoelectric and CO_2). Data was extracted from the Web of Science in May 2024. PEC: Photoelectrochemistry.

but their synergy also sparks a different kind of brilliance. Utilizing photoelectrochemistry (PEC) technology to convert CO_2 into fuel represents a new, clean, and green approach to using CO_2[1-3], which is increasingly attracting the interest of researchers [Figure 1]. Similar to other types of catalysis, the PEC conversion of CO_2 also involves multiple-step processes, resulting in a wide range of products such as C_1 (CO, CH_4, HCOOH, *etc.*) and C_{2+} products (C_2H_4, C_2H_6, CH_3COOH, *etc.*). Currently, most reported CO_2 conversion products are C_1 products because the generation of C_{2+} products involves a C-C coupling process, which is more difficult to obtain than C_1 products. But, compared with C_1 products, C_{2+} products have higher added value, and research on directly converting CO_2 into C_{2+} products holds significant significance. To date, several review articles have covered the overall research status on PEC CO_2 conversion[1-7], the influence of cocatalysts[8-10], the design of the PEC cathodes[11-15], the impact of PEC parameters[16,17], and the study of catalysts[18-20]. However, no individual summaries have been on converting CO_2 into C_{2+} products using the PEC technology. Hence, firstly, this paper aims to briefly introduce the basic principles of CO_2 conversion into C_{2+} products. Secondly, it summarizes the catalysts and reactor types reported thus far for obtaining C_{2+} products. Thirdly, it emphasizes the design strategies of catalysts currently available for generating or enhancing C_{2+} selectivity. Finally, it concludes with a summary of the current work and prospects for future research.

FUNDAMENTAL OF PHOTOELECTROCHEMICAL CO_2 REDUCTION

The PEC reduction of CO_2 involves light absorption, charge carrier transfer, CO_2 adsorption and activation, surface reactions, and product desorption. The energy input for PEC catalysis is provided by light and electricity. Light plays a role in generating high-energy photoelectrons for CO_2 reduction, generating photoelectric voltage to reduce energy consumption to some extent and lower economic costs, and producing heat to promote the progress of the reaction. Electricity plays a role in introducing an additional bias voltage to accelerate charge carrier separation and increase local charge density. By adjusting the bias voltage, the CO_2 reduction pathway can be altered to enhance selectivity.

Additionally, the supplementation of voltage can enable semiconductor materials that were originally not viable for photocatalytic CO_2 conversion to become feasible [Figure 1]. The synergistic effects of light and
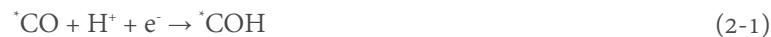
electricity can effectively reduce the activation energy for CO_2 reduction, but the study of the photoelectric synergistic effect is still lacking[21,22]. Furthermore, the contribution and distinction between photogenerated and voltage-provided electrons have not yet been reported.

Based on current reports, the mechanism for converting CO_2 into C_{2+} involves first converting CO_2 into $^*CO$ intermediates, followed by the generation of various intermediates of C_{2+} products through C-C coupling and multi-proton-coupled electron transfer (PCET), as shown by the equations for different pathways (Route 1-6)[23]. However, the competitive adsorption of $^*H_{ad}$ and $^*CO$ on monocomponent catalysts hinders the enhancement of PCET and C-C reaction kinetics. In order to break the linear scaling relationship between the adsorption of $^*H_{ad}/^*CO$ intermediates and improve water dissociation on auxiliary sites or CO_2-to-CO production, tandem catalysts consisting of multicomponents have been developed. These catalysts can achieve higher coverage of $^*H_{ad}$ and $^*CO$, which is more conducive to the generation of C_{2+} products. However, to our knowledge, while there are detailed reports on achieving C_{2+} products through serial pathways in the electrocatalytic conversion of CO_2[24], their application in the field of photoelectrocatalytic CO_2 conversion has not been observed.
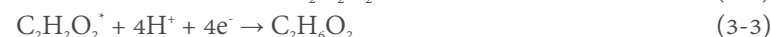
Route 1:

$$^*CO + H^+ + e^- \rightarrow {}^*COH \tag{1-1}$$
$$^*COH + 3H^+ + 3e^- \rightarrow {}^*CH_2 + H_2O \tag{1-2}$$
$$^*CH_2 + CO \rightarrow {}^*C_2H_2O \tag{1-3}$$
$$^*C_2H_2O + OH^- \rightarrow CH_3COO^- \tag{1-4}$$

Route 2:

$$^*CO + H^+ + e^- \rightarrow {}^*COH \tag{2-1}$$
$$^*COH + 3H^+ + 3e^- \rightarrow {}^*CH_2 + H_2O \tag{2-2}$$
$$^*CH_2 + H^+ + e^- \rightarrow {}^*CH_3 \tag{2-3}$$
$$2{}^*CH_3 \rightarrow C_2H_6 \tag{2-4}$$

Route 3:

$$^*CO + H^+ + e^- \rightarrow {}^*CHO \tag{3-1}$$
$$^*CHO + CO + H^+ + e^- \rightarrow C_2H_2O_2{}^* \tag{3-2}$$
$$C_2H_2O_2{}^* + 4H^+ + 4e^- \rightarrow C_2H_6O_2 \tag{3-3}$$

Route 4:

$$2{}^*CO + e^- \rightarrow {}^*CO\text{-}{}^*CO \tag{4-1}$$
$$^*CO\text{-}{}^*CO + H^+ \rightarrow {}^*CO\text{-}{}^*COH \tag{4-2}$$
$$^*CO\text{-}{}^*COH + 4H^+ + 4e^- \rightarrow CH_2CHO^* + H_2O \tag{4-3}$$
$$CH_2CHO^* + H^+ + e^- \rightarrow C_2H_4 + {}^*O \tag{4-4}$$

Route 5:

$$2{}^*CO + e^- \rightarrow {}^*CO\text{-}{}^*CO \tag{5-1}$$
$$^*CO\text{-}{}^*CO + H^+ \rightarrow {}^*CO\text{-}{}^*COH \tag{5-2}$$
$$^*CO\text{-}{}^*COH + 4H^+ + 4e^- \rightarrow CH_2CHO^* + H_2O \tag{5-3}$$
$$CH_2CHO^* + H^+ + e^- \rightarrow CH_3CHO^* \tag{5-4}$$
$$CH_3CHO^* + H^+ + e^- \rightarrow CH_3CH_2O^* \tag{5-5}$$
$$CH_3CH_2O^* + H^+ + e^- \rightarrow C_2H_5OH \tag{5-6}$$

Route 6:

$$2^*CO + e^- \rightarrow {}^*CO\text{-}^*CO \tag{6-1}$$
$${}^*CO\text{-}^*CO + H^+ \rightarrow {}^*CO\text{-}^*COH \tag{6-2}$$
$${}^*CO\text{-}^*COH + 4H^+ + 4e^- \rightarrow CH_2CHO^* + H_2O \tag{6-3}$$
$$CH_2CHO^* + H^+ + e^- \rightarrow CH_3CHO^* \tag{6-4}$$
$$CH_3CHO^* + 4H^+ + 4e^- + {}^*CO \rightarrow CH_3CH_2CHO^* + H_2O \tag{6-5}$$
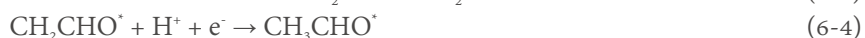$$CH_3CH_2CHO^* + 2H^+ + 2e^- \rightarrow n\text{-}C_3H_7OH \tag{6-6}$$

CATALYSTS AND REACTORS OF PHOTOELECTROCHEMICAL CO_2 UPGRADING TO C_{2+}

Hitherto, catalyst research for the PEC conversion of CO_2 into C_{2+} products is focused on photocathodes, primarily using Cu-based catalysts[21,24-29] [Table 1]. Cu-based species have a high binding affinity for $^*CO$ intermediates, making them active sites for CO_2 reduction and the generation of C_{2+} chemical species. However, the high energy barriers associated with C-C coupling and PCET processes still pose challenges for Cu-based catalysts regarding high overpotential and low selectivity towards C_{2+} products. In addition to Cu-based catalysts, reasonable structural design of some non-Cu-based catalysts enables higher selectivity towards C_{2+} products. Table 2 lists the selectivity of some non-Cu-based catalysts in photoelectrocatalytic CO_2 conversion. It shows that the non-Cu-based catalysts are mainly composite materials, including TiO_2, ZnO, WO_3, *etc.*, with more negative potentials compared to Cu-based catalysts. Regardless of Cu-based or non-Cu-based catalysts, ethanol, acetic acid, and ethylene are the main C_{2+} products; the yield of C_{2+} products is relatively low (typically at the μmol level); the Faradaic efficiencies cover a wide range, and the faradaic efficiency for a single C_{2+} product can reach up to 80%. The selectivity of C_{2+} products is primarily enhanced by adjusting the synthesis process of materials, doping with heteroatoms, and compositing with other metals/metal oxides/non-metallic materials to alter the morphology, band structure, and local electron density of the electrode materials.

In addition to catalysts, the selection of reactors also significantly influences the generation of C_{2+} products. The light source, membrane characteristics, electrolyte, manufacturing materials, wall thickness, operational modes (batch or flow), heat exchange, phase requirements (gas-solid, liquid-solid, or gas-liquid-solid), CO_2 solubility, and flow characteristics of feed gases and electrolytes can affect catalytic performance[54,55]. Currently, reactors used for CO_2 PEC conversion are primarily modified from electrochemical CO_2 reduction reactors and can be divided into H-type and flow electrolysis cells [Figure 2][56-58]. The H-type electrolysis cell is a relatively simple device that belongs to a batch reactor. It separates the anode and cathode using ion exchange membranes. However, its significant Ohmic resistance between the electrodes and limited CO_2 solubility have hindered its development. The low current density (< 100 mA·cm^{-2}) achieved in H-type cells does not meet industrial requirements. Furthermore, alkaline electrolytes are more conducive to suppressing H_2 reduction and enhancing C-C coupling. However, alkaline electrolytes are not feasible in aqueous CO_2 reduction conducted in H-type electrolysis cells. Nevertheless, the gas diffusion electrode (GDE) of the flow electrolysis cell separates the CO_2 flow field from the liquid electrolyte, allowing the use of high-concentration alkaline electrolytes.

The flow electrolysis cell is a continuous operation reactor where gases and electrolytes can be continuously supplied to the electrolytic cell. GDEs are used as the electrodes, which greatly overcome the limitations of CO_2 solubility. However, a certain distance between the anode and cathode still exists, resulting in significant Ohmic resistance. The membrane-electrode reactor integrates the anode, cathode, and membrane assembly, significantly reducing the distance between the electrodes and exhibiting improved catalytic performance. However, it lacks a reference electrode, making it challenging to obtain accurate working electrode potentials. Although membrane-electrode reactors have found wide applications in

Table 1. Selected Cu-based catalyst for photoelectrochemical conversion of CO_2 to C_{2+}

Photoelectrode	Electrolyte	Light source1111	Potential	C_{2+} products	Ref.
Cu@porphyrin-COFs	$KHCO_3$ (0.5 M)	300 W Xenon lamp (200 $mW \cdot cm^{-2}$)	-1.0 V *vs.* SCE	Ethanol + acetic acid + acetone (~27 $\mu mol \cdot h^{-1} \cdot cm^{-2}$)	[30]
$Zn_{0.2}:Co_1@Cu$	$KHCO_3$ (0.1 M), Eosin Y (0.01 M)	AM 1.5G (200 $mW \cdot cm^{-2}$)	-0.4 V *vs.* SCE	Paraffin (325 $\mu g \cdot h^{-1}$)	[31]
$CuBi_2O_4/TiO_2$-NTs	$NaHCO_3$ (0.1 M)	250 W Xenon lamp (200 $mW \cdot cm^{-2}$)	-0.6 V *vs.* SCE	Ethanol (1.32 $\mu mol \cdot h^{-1}$) (FE 73%)	[32]
6 wt% Re-doped CuO/ TiO_2-NTs	$NaHCO_3$ (0.1 M)	300 W Xenon lamp	-0.5 V *vs.* SCE	Ethanol (1.9 $\mu mol \cdot h^{-1}$)	[33]
CZTS/CdS	$KHCO_3$ (0.1 M)	AM 1.5G (100 $mW \cdot cm^{-2}$)	-0.4 V *vs.* RHE	Ethanol (~2.5 $\mu mol \cdot h^{-1} \cdot cm^{-2}$)	[34]
TiO_2-NT/GNR/Cu/Pd-Pt	Na_2SO_4 (0.1 M)	150 W Xenon lamp	-0.7 V *vs.* Ag/AgCl	Ethanol (4.3 $mmol \cdot g^{-1} \cdot h^{-1} \cdot cm^{-2}$)	[35]
$GO/Cu_xO/Cu$-BTC	$KHCO_3$ (0.1 M), Na_2SO_4 (0.1 M)	AM 1.5G (100 $mW \cdot cm^{-2}$)	-0.5 V *vs.* Ag/AgCl	Ethanol (40.5 $\mu mol \cdot h^{-1} \cdot cm^{-2}$)	[36]
Cu	KOH (1 M)	UV LED lights (365 nm, 100 $mW \cdot cm^{-2}$)	-1.8 V *vs.* Ag/AgCl	Ethylene (4.7 $\mu mol \cdot s^{-1} \cdot m^{-2}$) (FE 46.6%)	[37]
CuN_x/CuO	$KHCO_3$ (0.1 M)	AM 1.5G (100 $mW \cdot cm^{-2}$)	0.2V *vs.* RHE	Ethanol (13.7 $\mu mol \cdot h^{-1} \cdot cm^{-2}$) (FE 15.2%)	[38]
CuO-$CuFeO_2$	H_2O: triethanolamine (volume ratio of 9:1)	300 W Xenon lamp (100 $mW \cdot cm^{-2}$)	-0.6 V *vs.* Ag/AgCl	Ethanol (FE 66.73%)	[39]
Cu/TiO_2/p-Si	$CsHCO_3$ (0.1 M)	300 W Xenon lamp, AM 1.5G (100 $mW \cdot cm^{-2}$)	-0.9 V *vs.* RHE	Ethylene (FE ~23%)	[40]

COFs: Covalent organic frameworks; SCE: saturated calomel electrode; FE: Faradaic efficiency; RHE: reversible hydrogen electrode; UV LED: ultraviolet light-emitting diode.

electrochemical CO_2 reduction, there are few reports on their use in photoelectrochemical CO_2 conversion[37]. In addition, the state-of-the-art electrocatalytic CO_2 reduction performance achieved from flow electrolysis cells and membrane-electrode electrolyzers can almost produce CO and formic acid at industrial current densities. However, producing single high-value C_{2+} products, such as ethylene and ethanol, remains challenging. As for photoelectrochemical CO_2 reduction, the current densities used in the electrolytic cells have a significant gap compared to industrial current densities. It is worth mentioning that most of the recent research employs self-designed, assembled, or customized CO_2 photoelectrochemical reactors. No universally recognized standard exists for the configuration and operation of CO_2 electrolyzers. Different studies use distinct reactor structures, components, and catalysts, making it difficult to directly compare results and select optimal cathodic catalysts.

STRATEGIES TO IMPROVE THE SELECTIVITY OF C_{2+} PRODUCTS

The photoelectrochemical conversion of CO_2 into C_{2+} products is highly challenging. The entire process involves multiple aspects: absorption of light to obtain electron-hole pairs, followed by charge separation and transfer to the surface of the photocathode. At the same time, CO_2 adsorption is necessary for reducing CO_2 to form C_1 radicals and intermediates, and the stability of intermediates and C-C coupling is crucial. Moreover, the production of C_{2+} products requires more electrons compared to C_1 products. These processes indicate that improving light absorption, enhancing CO_2 adsorption capacity, increasing charge separation and transfer efficiency, and constructing suitable active sites are essential for obtaining high-content C_{2+} products. In addition, the reactor configuration, operating conditions, and electrode assembly also significantly influence catalytic performance. A continuous flow PEC reactor can produce more C_2-C_3 products compared to batch reactors[58], and selecting an appropriate voltage is beneficial for the generation of C_{2+} products[17]; appropriate electrode assembly can increase CO_2 adsorption, suppress hydrogen production, and facilitate C_{2+} product generation[40]. However, there is a lack of research on the impact of reactor configuration, operating conditions, and electrode assembly on the obtained C_{2+} products. Besides,

Table 2. The selected non-Cu-based catalyst for photoelectrochemical conversion of CO_2 to C_{2+}

Photoelectrode	Electrolyte111	Light source	Potential	C_{2+} products	Ref.
Ti/TiO$_2$NT-ZIF-8	Ascorbic acid (0.2 M), sodium sulfate (0.1 M)	125 W high pressure mercury vapor lamp	0.1 V $vs.$ Ag/AgCl (E_{app})	Ethanol (10.5 mmol·L^{-1})	[41]
CsPbBr$_3$/graphite (C)	KHCO$_3$ (0.1 M)	-	-0.8 V $vs.$ Ag/AgCl	Oxalic acid (3.44 × 10^{-5} mmol) (FE 44%)	[42]
Dye/Pd/N-TiO$_2$	KHCO$_3$ (0.1 M), Eosin Y (1 mM)	300 W Xenon lamp (200 mW·cm^{-2})	-1.0 V	Ethanol (26.8 µmol·h^{-1}·cm^{-2}) (FE 28.4%)	[43]
ZnO/Ni-30	KHCO$_3$ (0.1 M), Eosin Y (1 mM)	300 W Xenon lamp (100 mW·cm^{-2})	-0.6 V	Ethanol + acetic acid (12.5 µmol·h^{-1}·cm^{-2}) (FE 100%)	[44]
Pd-TiO$_2$@ZnO	KHCO$_3$ (0.1 M), Eosin Y (1 mM)	300 W Xenon lamp (200 mW·cm^{-2})	-1.0 V	Ethanol + acetic acid (~30 µmol·h^{-1}·cm^{-2})	[45]
Bi$_2$WO$_6$/BiOCl	KHCO$_3$ (0.1 M), Eosin Y (1 mM)	300 W Xenon lamp	-1.0 V	Ethanol (11.4 µmol·h^{-1}·cm^{-2}) (FE 80%)	[46]
S-TiO$_2$@GS	KHCO$_3$ (0.1 M), Eosin Y (1 mM)	300 W Xenon lamp (200 mW·cm^{-2})	-0.9 V $vs.$ SCE	Ethanol (20.7 µmol·h^{-1}·cm^{-2})	[47]
P-WO$_3$	KHCO$_3$ (0.1 M), Eosin Y (1 mM)	300 W Xenon lamp (200 mW·cm^{-2})	-0.8 V $vs.$ SCE	Acetic acid (4.7 µmol·L^{-1}·h^{-1}·cm^{-2})	[48]
CdS/V$_S$-MoS$_2$-PS	KHCO$_3$ (0.1 M), Na$_2$SO$_3$ (0.1 M), Eosin Y (1 mM)	200 mW·cm^{-2}	-0.9 V $vs.$ SCE	Ethanol + ethylene glycol (350 µmol·h^{-1}·cm^{-2}) (FE 67%)	[49]
Pd@TiO$_2$/Ti$_3$CN	KHCO$_3$ (0.1 M)	300 W Xenon lamp	-0.8 V	Ethanol (14 µmol·h^{-1}·cm^{-2})	[50]
Pd/R-TiO$_2$/TiN-30	KHCO$_3$ (0.1 M), Eosin Y (1 mM)	300 W Xenon lamp (200 mW·cm^{-2})	-0.8 V $vs.$ SCE	Ethanol + acetic acid + glycolaldehyde (39.41 µmol·L^{-1}·h^{-1}·cm^{-2}) (FE 65.69%)	[51]
NiMoO$_4$/ZnO-3	Na$_2$SO$_3$ (0.1 M)	Xenon lamp (100 mW·cm^{-2})	-0.8 V $vs.$ SCE	Ethanol + acetic acid + glycolaldehyde + ethylene glycol (29.2 µmol·h^{-1}·cm^{-2}) (FE 72.6%)	[52]
Si@WO$_3$-NS	KHCO$_3$ (0.1 M)	300 W Xenon lamp (100 mW·cm^{-2})	-1.0 V $vs.$ SCE	Acetone + ethanol + acetic acid + glycolaldehyde (~43 µmol·h^{-1}·cm^{-2}) (FE 62.7%)	[53]

FE: Faradaic efficiency; SCE: saturated calomel electrode; NS: nanosheet.

the current yield of C_{2+} products from CO_2 conversion via photoelectrocatalysis is generally low (often below 50 µmol·cm^{-2}·h^{-1}), with correspondingly low current densities (below 10 mA·cm^{-2}); many studies do not report CO_2 conversion rates or product yields[25]. According to the reaction process, conversion rates and yields can be enhanced by adjusting reactor and reaction parameters (such as applying pressure) and modifying the properties of the photoelectrode. Specifically, improving light absorption capacity (through morphology control and elemental doping, *etc.*), enhancing charge carrier separation (via auxiliary metal addition and defect or heterojunction construction, *etc.*), and promoting surface reactions (by depositing a thin bilayer of Sustainion/Nafion, *etc.*) can contribute to these enhancements[4]. Therefore, this section mainly summarizes the research progress in improving the selectivity of C_{2+} products from four aspects: electrode material morphology design, adjustment of band structure, construction of heterojunctions, and design of active sites.

Morphology

The morphology significantly influences the selectivity of CO_2 PEC reduction products [Figure 3]. Current research suggests that C_{2+} products can be acquired by constructing specific spatial structures. Wang *et al.* found that three-dimensional (3D) nanorod-shaped zinc oxide exhibited the optimal spatial environment compared to amorphous block-, mushroom-, and ball cactus-like structures, facilitating C-C coupling to produce C_2 products (ethanol and acetic acid)[44]. Furthermore, their research group discovered that porous PEC based on a 3D hierarchical structure of covalent organic frameworks (COFs) could effectively enhance
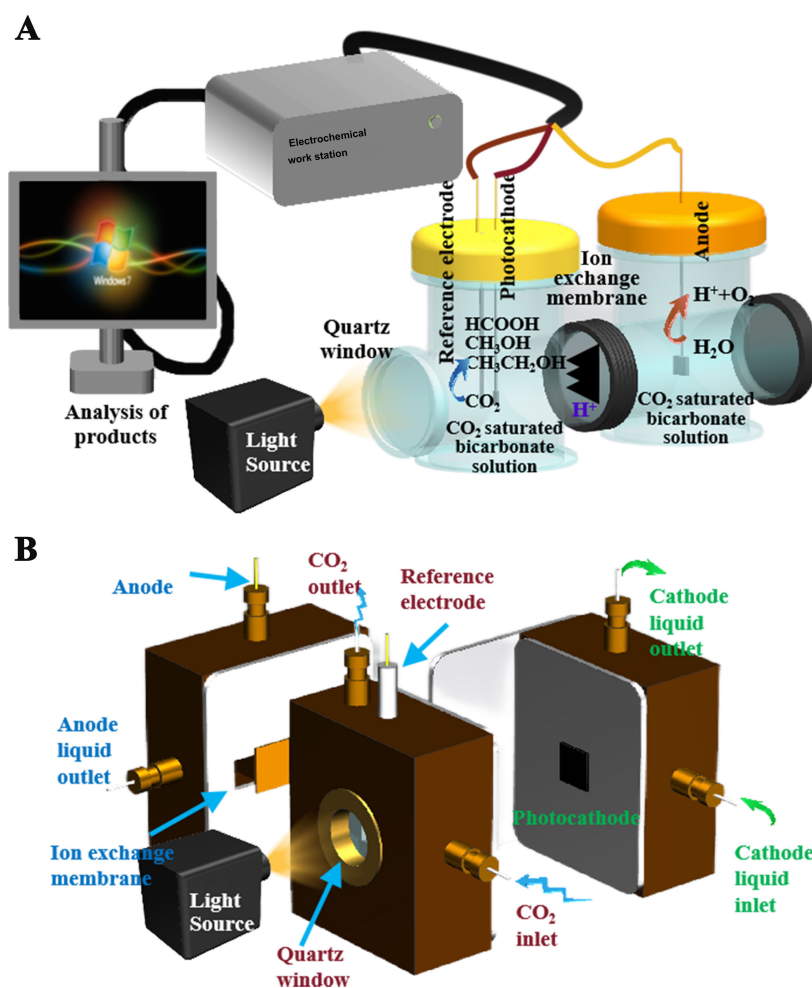
Figure 2. PEC reactor for CO_2 conversion (A) H-type cell (batch reactor)[54];(B) flow cell (continuous reactor). PEC: Photoelectrochemistry.

CO_2 adsorption and the rate of C-C coupling to generate C_{2+} products[30]. Hollow catalysts exhibited different selectivity on the inner and outer surfaces due to the increased collision probability of intermediates within the closed cavity, achieving a high selectivity of C_{2+} products (67.0%) on the inner surface[49]. In addition, by simulating the morphology of thylakoids in plant cells, the Si@WO_3-nanosheet (NS) catalyst with a 2D-3D structure is advantageous for achieving C-C coupling[53].

Band structure

The band structure of electrode materials significantly influences light utilization and the types of CO_2 reduction products. A narrower band gap is beneficial for broadening the absorption range of light. In contrast, adjustable conduction band positions facilitate the control of product selectivity [Figure 4]. The position of the conduction band is related to the reduction capability of the catalyst, playing a crucial role in the photoelectrocatalytic reduction of CO_2 and serving as a thermodynamic factor influencing the availability of C_{2+} products. Adjusting the conduction band to the appropriate position is beneficial for improving the acquisition of certain C_{2+} products. Han *et al.* achieved improved selectivity of CO_2 reduction products by depositing metals such as Pd, Pt, Ni, Au, *etc.*, to modulate the conduction band potentials of the TiO_2@ZnO/FTO[45]. Besides doping with metals, doping with non-metals can alter the conduction band
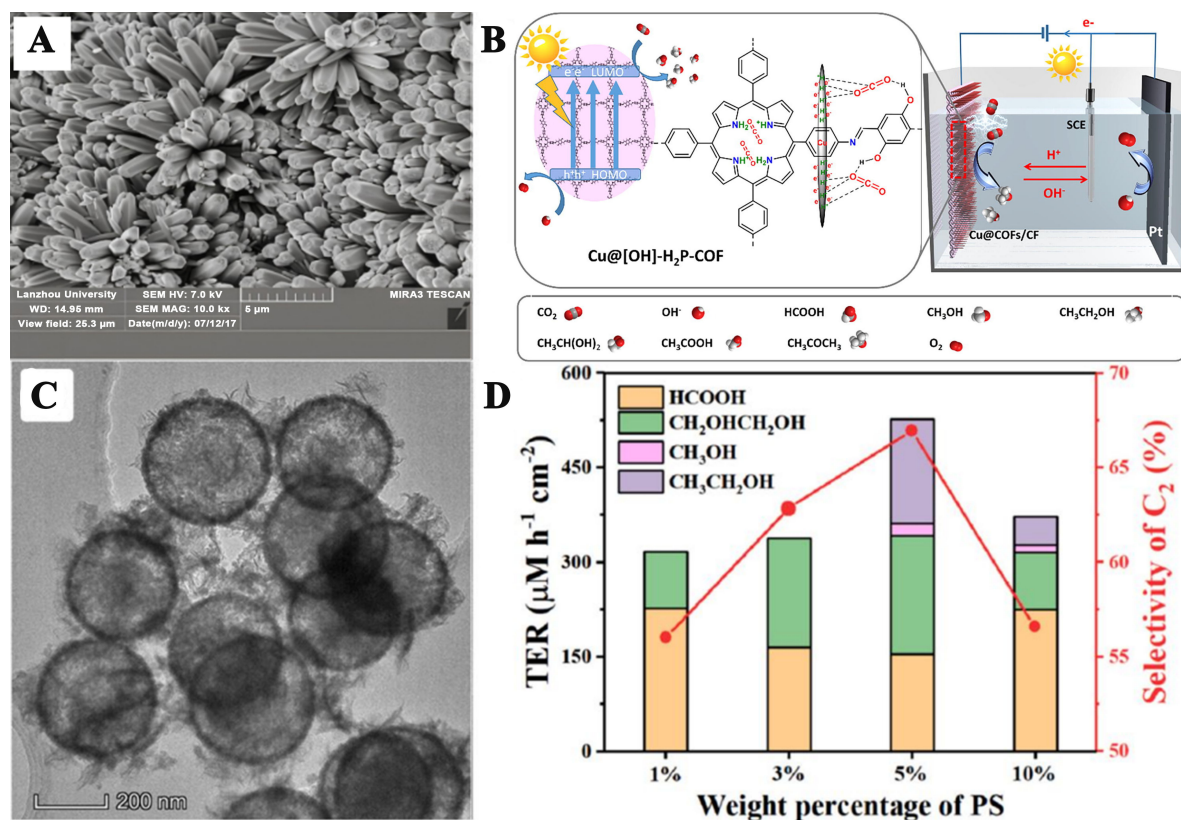
Figure 3. (A) SEM image of 3D nanorod ZnO[44].Copyright 2018 Springer; (B) COFs-based porous photoelectrochemical with 3D hierarchical structure for CO_2 reduction[30].Copyright 2020 Elsevier; (C) TEM image of CdS/V_S-MoS_2 and (D) catalytic performance of CdS/V_S-MoS_2-PS[49].Copyright 2023 Elsevier. SEM: Scanning electron microscopy; 3D: three-dimensional; COFs: covalent organic frameworks; TEM: transmission electron microscopy.
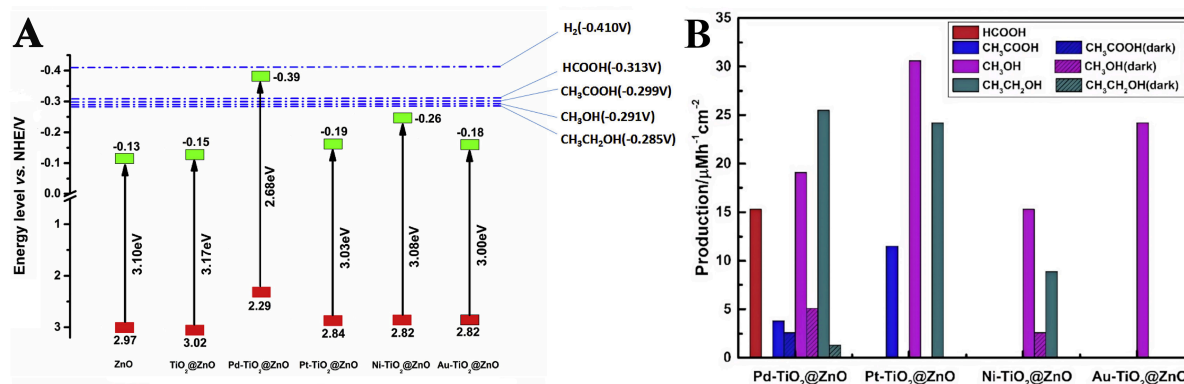

Figure 4. (A) Band structure of samples; (B) CO_2 PEC performance of the samples[45].Copyright 2018 Elsevier. PEC: Photoelectrochemistry.

position. Yu *et al.* designed and prepared a novel P-doped WO_3 catalyst where P doping elevated the conduction band position of the WO_3 electrode from -0.13 to -0.54 V [V *vs.* normal hydrogen electrode (NHE)], achieving an acetic acid yield of 4.7 μmol/(L·h·cm²) at a conduction band position of -0.38 V (V *vs.* NHE)[48].
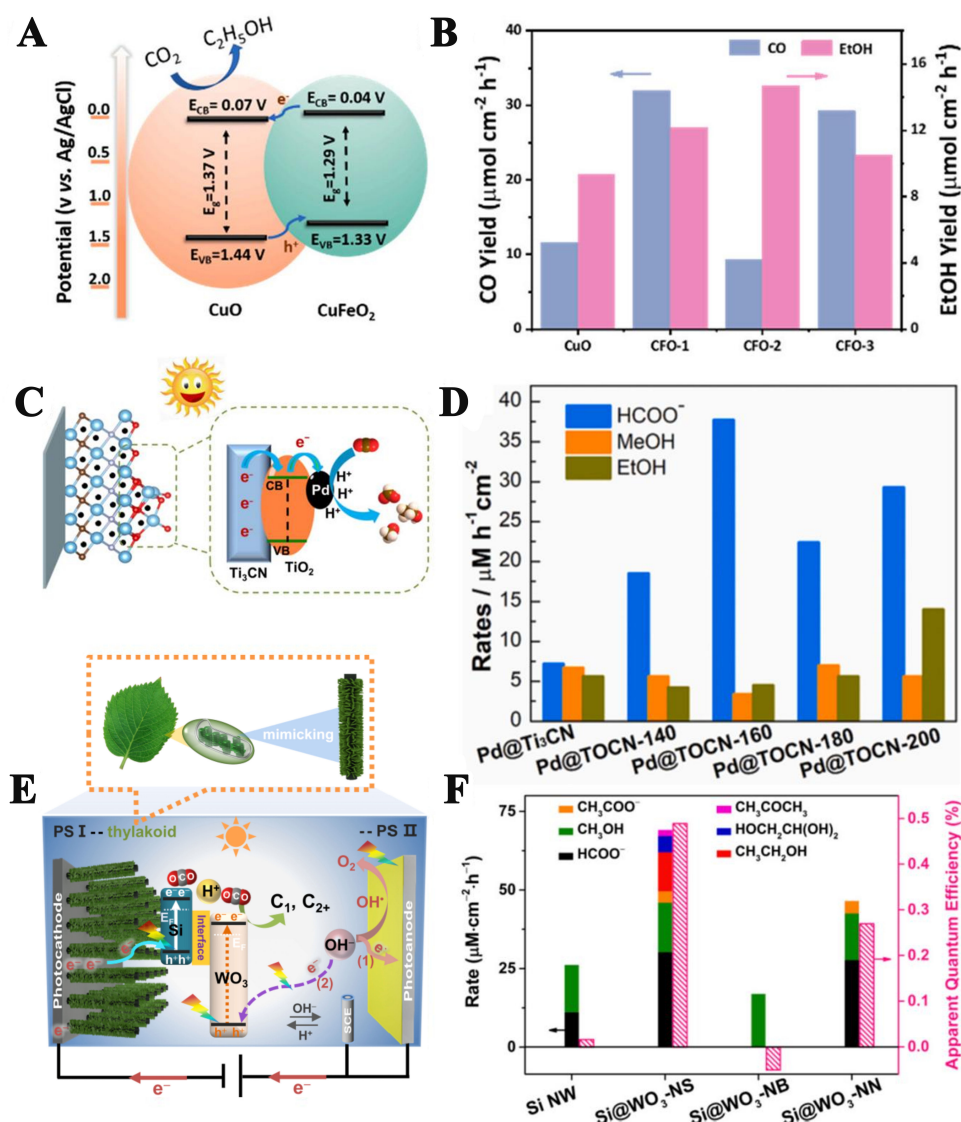
Figure 5. (A) Band structure of CuO-$CuFeO_2$; (B) CO_2 PEC performance of samples at -1.0 V *vs*. Ag/AgCl[39]. Copyright 2023 Elsevier; (C) Band structure of Pd@TOCN; (D) CO_2 PEC performance of samples[50]. Copyright 2023 Elsevier; (E) Band structure of Si@WO_3 and (F) CO_2 PEC performance of samples[53]. Copyright 2023 Elsevier. PEC: Photoelectrochemistry.

Heterojunction

The built-in electric field of heterojunctions facilitates carrier separation, accelerates charge transfer, and enhances the velocity of intermediates, resulting in a high probability of C-C coupling and, consequently, higher C_{2+} product yields[31,53] [Figure 5]. Lu *et al*. constructed 0D/1D $CuFeO_2$/CuO nanowire heterojunction arrays. They achieved a higher Faradaic efficiency (66.73%) for ethanol production at -0.6 V *vs*. Ag/AgCl, mainly attributed to the rapid separation of photogenerated electrons and holes in the heterojunction material and the transfer of electrons from $CuFeO_2$ to CuO, enabling highly content of C_{2+} products (ethanol)[39]. Xu *et al*. fabricated 2D TiO_2/Ti_3CN MXene heterojunctions, where the Pd@TOCN-200 photoelectrode exhibited the highest ethanol production rate (14 $\mu M \cdot cm^{-2} \cdot h^{-1}$) due to the enhanced CO_2 adsorption and favorable C-C coupling environment provided by the 2D TiO_2/Ti_3CN heterojunction structure[50].
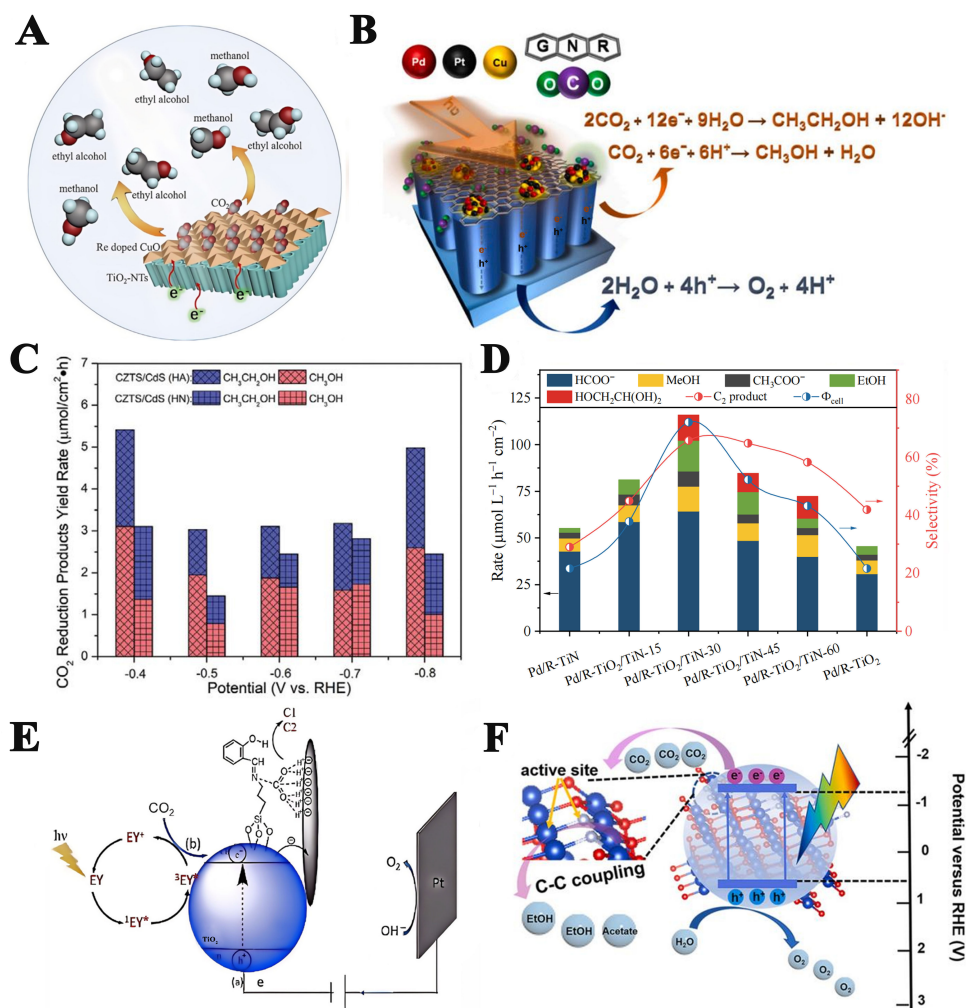
Figure 6. (A) Schematic mechanism of Re-doped CuO/TiO$_2$-NTs for CO$_2$ reduction[33]. Copyright 2021 Elsevier; (B) The scheme for product generation of TiO$_2$-NT/GNR-metal electrodes[35]. Copyright 2021 Elsevier; (C) The corresponding CO$_2$ conversion yields of CZTS/CdS (HA) and CZTS/CdS (HN)[34]. Copyright 2021 Wiley; (D) CO$_2$ PEC performance of Pd/R-TiO$_2$/TiN- x[51]. Copyright 2023 Elsevier; (E) Schematic mechanism of EY+S-TiO$_2$@GS for CO$_2$ reduction[47]. Copyright 2020 Elsevier; and (F) Schematic mechanism of CuN$_x$/CuO for the CO$_2$ PEC reduction[38]. Copyright 2022 Elsevier. PEC: Photoelectrochemistry.

Active site

The active site is a critical part of catalytic reactions and directly determines the distribution of products. They change product distribution by affecting the adsorption strength of products and intermediates and promote the coupling of *CO with *CO by adjusting the local electron density gradient, facilitating C-C coupling, and enhancing the acquisition of C$_{2+}$ products. In the PEC CO$_2$ reduction reaction, active sites composed of multimetallic species[31,33,35,36,52], oxygen vacancies/sulfur vacancies[34,51], certain specific functional groups (such as adjacent imine groups)[47], and metal-nonmetal junctions[38] are favorable for CO$_2$ adsorption and C-C coupling, promoting the generation of C$_{2+}$ products [Figure 6]. Among them, Lu *et al.* doped Re into CuO and combined it with Ti nanotubes. Under solar light and -0.5 V *vs.* saturated calomel electrode (SCE) conditions, the product was almost entirely ethanol (1.9 μM·h^{-1}). The above results were attributed to high-valence rhenium as an active site for hydrogenation reactions. Its doping promoted the alcoholization process and facilitated C-C coupling[33]. Zhou *et al.* adjusted the surface sulfur vacancies of Cu$_2$ZnSnS$_4$ (CZTS)/CdS by annealing in different atmospheres, which were active sites for CO adsorption and followed C-C coupling. By rational tuning, they achieved higher ethanol selectivity[34]. In addition,

Wang *et al.* introduced N into CuO to obtain Cu-N active components. These components possessed asymmetric d-p orbitals, which could reduce the activation energy of C-C coupling and induce local charge redistribution, thereby improving the material's conductivity. They achieved a 15.2% C_2 product selectivity in a water solution at 0.2 V *vs*. reversible hydrogen electrode (RHE)[38].

CONCLUSION AND PROSPECTS

Currently, research on PEC conversion of CO_2 to C_{2+} products primarily focuses on developing photoelectrodes. The catalysts used are mainly Cu-based, and the major C_{2+} products obtained are ethanol, acetic acid, and ethylene. The involved reactors are predominantly flow reactors. Adjusting the catalyst morphology, band structure, and active sites can improve light absorption, enhance charge carrier transfer, strengthen CO_2/CO^* adsorption, and provide a favorable C-C coupling environment, achieving high selectivity for C_{2+} products. Although some progress has been made in the research on PEC CO_2 conversion to C_{2+} products, there is currently limited reporting on products containing three or more carbon atoms. The types of catalysts used are also limited, and their yields are relatively low (typically at the level of μmol). The reactors used in studies are mostly self-designed, assembled, or customized. There is no recognized standard for the configuration and operation of CO_2 reactors, and it is difficult to selectively optimize cathode catalysts by directly comparing different research reports. The current density employed in electrolytic cells differs significantly from industrial-scale requirements, making industrialization challenging. The present reaction pathway is not yet clear, and there is still insufficient research on the specific reaction mechanisms involved in catalysts. Additionally, research on photoelectric synergies is lacking. Therefore, increasing efforts in reactor development and establishing design standards, exploring and developing cost-effective and high-performing catalysts, and conducting in-depth research to enhance catalytic performance and understand reaction mechanisms are the main directions for future investigations.

DECLARATIONS

Authors' contributions
Prepared and revised the manuscript: Jiang X, Chen R
Designed and revised the manuscript: Chen YX, Lu CZ
All authors contributed to the discussion and preparation of the manuscript.

Availability of data and materials
Not applicable.

Conflicts of interest
Chen YX is both the Junior Editorial Board Member of *Chemical Synthesis* and the guest editor of the Special Issue "Synthesis of Advanced Material for Novel Fuel Cells", while the other authors have declared that they have no conflicts of interest.

Ethical approval and consent to participate

Not applicable.

Consent for publication

Not applicable.

Copyright

© The Author(s) 2024.

REFERENCES

1. Zhou W, Guo JK, Shen S, et al. Progress in photoelectrocatalytic reduction of carbon dioxide. *Acta Phys Chim Sin* 2020;36:1906048. DOI

2. Tang B, Xiao FX. An overview of solar-driven photoelectrochemical CO_2 Conversion to chemical fuels. *ACS Catal* 2022;12:9023-57. DOI

3. Xu S, Shen Q, Zheng J, et al. Advances in biomimetic photoelectrocatalytic reduction of carbon dioxide (Adv. Sci. 31/2022). *Adv Sci* 2022;9:2270196. DOI PMC

4. Chen P, Zhang Y, Zhou Y, Dong F. Photoelectrocatalytic carbon dioxide reduction: fundamental, advances and challenges. *Nano Mater Sci* 2021;3:344-67. DOI

5. Zhang N, Long R, Gao C, Xiong Y. Recent progress on advanced design for photoelectrochemical reduction of CO_2 to fuels. *Sci China Mater* 2018;61:771-805. DOI

6. Ochedi FO, Liu D, Yu J, Hussain A, Liu Y. Photocatalytic, electrocatalytic and photoelectrocatalytic conversion of carbon dioxide: a review. *Environ Chem Lett* 2021;19:941-67. DOI

7. Kan M, Wang Q, Hao S, et al. System engineering enhances photoelectrochemical CO_2 reduction. *J Phys Chem C* 2022;126:1689-700. DOI

8. Chang X, Wang T, Yang P, Zhang G, Gong J. The development of cocatalysts for photoelectrochemical CO_2 reduction. *Adv Mater* 2019;31:e1804710. DOI PubMed

9. Dutta S, Patil R, Chongdar S, Bhaumik A. Dehydrogenase-functionalized interfaced materials in electroenzymatic and photoelectroenzymatic CO_2 reduction. *ACS Sustain Chem Eng* 2022;10:6141-56. DOI

10. Li Y, Li S, Huang H. Metal-enhanced strategies for photocatalytic and photoelectrochemical CO_2 reduction. *Chem Eng J* 2023;457:141179. DOI

11. Liu L, Zhang Y, Huang H. Junction engineering for photocatalytic and photoelectrocatalytic CO_2 reduction. *Solar RRL* 2021;5:2000430. DOI

12. Brillas E, Serrà A, Garcia-segura S. Biomimicry designs for photoelectrochemical systems: Strategies to improve light delivery efficiency. *Curr Opin Electrochem* 2021;26:100660. DOI

13. Devi P, Verma R, Singh JP. Advancement in electrochemical, photocatalytic, and photoelectrochemical CO_2 reduction: recent progress in the role of oxygen vacancies in catalyst design. *J CO2 Util* 2022;65:102211. DOI

14. Putri LK, Ng BJ, Ong WJ, Chai SP, Mohamed AR. Toward excellence in photocathode engineering for photoelectrochemical CO_2 reduction: design rationales and current progress. *Adv Energy Mater* 2022;12:2201093. DOI

15. Li Y, Li S, Huang H. Defective photocathode: fundamentals, construction, and catalytic energy conversion. *Adv Funct Mater* 2023;33:2304925. DOI

16. Pawar AU, Kim CW, Nguyen-le M, Kang YS. General review on the components and parameters of photoelectrochemical system for CO_2 reduction with in situ analysis. *ACS Sustainable Chem Eng* 2019;7:7431-55. DOI

17. King AJ, Bui JC, Bell AT, Weber AZ. Establishing the role of operating potential and mass transfer in multicarbon product generation for photoelectrochemical CO_2 reduction cells using a Cu catalyst. *ACS Energy Lett* 2022;7:2694-700. DOI

18. Verma S, Yadav A. Emerging single-atom catalysts and nanomaterials for photoelectrochemical reduction of carbon dioxide to value-added products: a review of the current state-of-the-art and future perspectives. *Energy Fuels* 2023;37:5712-42. DOI

19. Hiragond CB, Kim J, Kim H, Bae D, In S. Elemental-doped catalysts for photoelectrochemical CO_2 conversion to solar fuels. *Solar RRL* 2024;8:2400022. DOI

20. Bienkowski K, Solarska R, Trinh L, et al. Halide perovskites for photoelectrochemical water splitting and CO_2 reduction: challenges and opportunities. *ACS Catal* 2024;14:6603-22. DOI

21. Li CF, Guo RT, Zhang ZR, Wu T, Pan WG. Converting CO_2 into value-added products by Cu_2O-based catalysts: from photocatalysis, electrocatalysis to photoelectrocatalysis. *Small* 2023;19:e2207875. DOI PubMed

22. Zhang W, Jin Z, Chen Z. Rational-designed principles for electrochemical and photoelectrochemical upgrading of CO_2 to value-added chemicals. *Adv Sci* 2022;9:e2105204. DOI PubMed PMC

23. Zheng Y, Vasileff A, Zhou X, Jiao Y, Jaroniec M, Qiao SZ. Understanding the roadmap for electrochemical reduction of CO_2 to multi-carbon oxygenates and hydrocarbons on copper-based catalysts. *J Am Chem Soc* 2019;141:7646-59. DOI PubMed

24. Zheng W, Yang X, Li Z, et al. Designs of tandem catalysts and cascade catalytic systems for CO_2 upgrading. *Angew Chem Int Ed Engl*

2023;62:e202307283. DOI PubMed

25. Han GH, Bang J, Park G, et al. Recent advances in electrochemical, photochemical, and photoelectrochemical reduction of CO_2 to C_{2+} products. *Small* 2023;19:e2205765. DOI PubMed

26. Otgonbayar Z, Yoon CM, Oh WC. Photoelectrocatalytic CO_2 reduction with ternary nanocomposite of MXene (Ti_3C_2)-Cu_2O-Fe_3O_4: comprehensive utilization of electrolyte and light-wavelength. *Chem Eng J* 2023;464:142716. DOI

27. Landaeta E, Kadosh NI, Schultz ZD. Mechanistic study of plasmon-assisted *in situ* photoelectrochemical CO_2 reduction to acetate with a Ag/Cu_2O nanodendrite electrode. *ACS Catal* 2023;13:1638-48. DOI

28. Liang H, Li M, Li Z, Xie W, Zhang T, Wang Q. Photoelectrochemical CO_2 reduction with copper-based photocathodes. *J CO2 Util* 2024;79:102639. DOI

29. Guo X, Wang C, Yang Z, Yang Y. Boosting C_{2+} production from photoelectrochemical CO_2 reduction on gallium doped Cu_2O. *Chem Eng J* 2023;471:144539. DOI

30. Wang B, Yang F, Dong Y, et al. Cu@porphyrin-COFs nanorods for efficiently photoelectrocatalytic reduction of CO_2. *Chem Eng J* 2020;396:125255. DOI

31. Wang J, Guan Y, Yu X, et al. Photoelectrocatalytic reduction of CO_2 to paraffin using p-n heterojunctions. *iScience* 2020;23:100768. DOI PubMed PMC

32. Cao H, Yu H, Lu Y, et al. Photoelectrocatalytic reduction of CO_2 over $CuBi_2O_4$/TiO_2-NTs under simulated solar irradiation. *ChemistrySelect* 2020;5:5137-45. DOI

33. Lu Y, Cao H, Xu S, et al. CO_2 photoelectroreduction with enhanced ethanol selectivity by high valence rhenium-doped copper oxide composite catalysts. *J Colloid Interface Sci* 2021;599:497-506. DOI PubMed

34. Zhou S, Sun K, Huang J, et al. Accelerating electron-transfer and tuning product selectivity through surficial vacancy engineering on CZTS/CdS for photoelectrochemical CO_2 reduction. *Small* 2021;17:e2100496. DOI

35. de Souza MKR, Cardoso EDSF, Fortunato GV, et al. Combination of Cu-Pt-Pd nanoparticles supported on graphene nanoribbons decorating the surface of TiO_2 nanotube applied for CO_2 photoelectrochemical reduction. *J Environ Chem Eng* 2021;9:105803. DOI

36. Nandal N, Prajapati PK, Abraham BM, Jain SL. CO_2 to ethanol: a selective photoelectrochemical conversion using a ternary composite consisting of graphene oxide/copper oxide and a copper-based metal-organic framework. *Electrochim Acta* 2022;404:139612. DOI

37. Merino-garcia I, Castro S, Irabien A, et al. Efficient photoelectrochemical conversion of CO_2 to ethylene and methanol using a Cu cathode and TiO_2 nanoparticles synthesized in supercritical medium as photoanode. *J Environ Chem Eng* 2022;10:107441. DOI

38. Wang K, Liu Y, Wang Q, et al. Asymmetric Cu-N sites on copper oxide photocathode for photoelectrochemical CO_2 reduction towards C_2 products. *Appl Catal B Environ* 2022;316:121616. DOI

39. Lu M, Jia D, Xue H, Tian J, Jiang T. 0D/1D $CuFeO_2$/CuO nanowire heterojunction arrays for improved photoelectrocatalytic reduction of CO2 to ethanol. *J Alloys Compd* 2023;960:170626. DOI

40. Kim C, King AJ, Aloni S, Toma FM, Weber AZ, Bell AT. Codesign of an integrated metal-insulator-semiconductor photocathode for photoelectrochemical reduction of CO_2 to ethylene. *Energy Environ Sci* 2023;16:2968-76. DOI

41. Cardoso J, Stulp S, de Souza M, et al. The effective role of ascorbic acid in the photoelectrocatalytic reduction of CO_2 preconcentrated on TiO_2 nanotubes modified by ZIF-8. *J Electroanal Chem* 2020;856:113384. DOI

42. Bergamini L, Sangiorgi N, Gondolini A, et al. $CsPbBr_3$/platinum and $CsPbBr_3$/graphite hybrid photoelectrodes for carbon dioxide conversion to oxalic acid. *Solar Energy* 2023;254:213-22. DOI

43. Zhang Y, Han B, Xu Y, et al. Artificial photosynthesis of alcohols by multi-functionalized semiconductor photocathodes. *ChemSusChem* 2017;10:1742-8. DOI

44. Wang J, Han B, Nie R, et al. Photoelectrocatalytic reduction of CO_2 to chemicals via ZnO@Nickel foam: controlling C-C coupling by ligand or morphology. *Top Catal* 2018;61:1563-73. DOI

45. Han B, Wang J, Yan C, et al. The photoelectrocatalytic CO_2 reduction on TiO_2@ZnO heterojunction by tuning the conduction band potential. *Electrochim Acta* 2018;285:23-9. DOI

46. Wang J, Wei Y, Yang B, Wang B, Chen J, Jing H. In situ grown heterojunction of Bi_2WO_6/BiOCl for efficient photoelectrocatalytic CO_2 reduction. *J Catal* 2019;377:209-17. DOI

47. Wang L, Wei Y, Fang R, et al. Photoelectrocatalytic CO_2 reduction to ethanol via graphite-supported and functionalized TiO_2 nanowires photocathode. *J Photochem Photobiol A Chem* 2020;391:112368. DOI

48. Yu X, Wei Y, Chen Y, Wang J, Jing H. P-doped WO_3 semiconductor with enhanced conduction band on highly efficient photoelectrocatalytic reduction of CO_2. *Chinese Sci Bull* 2020;66:825-32. DOI

49. Liu C, Xiao Y, Wan W, et al. Different behaviors on the external and inner surface of hollow CdS/V_S-MoS_2 heterojunctions in photoelectrocatalytic CO_2 reduction via SH-assisted mechanism. *Appl Catal B Environ* 2023;325:122394. DOI

50. Xu Y, Wang F, Lei S, et al. In situ grown two-dimensional TiO_2/Ti_3CN MXene heterojunction rich in Ti^{3+} species for highly efficient photoelectrocatalytic CO_2 reduction. *Chem Eng J* 2023;452:139392. DOI

51. Wei Y, Duan R, Zhang Q, et al. Photoelectrocatalytic reduction of CO_2 catalyzed by TiO_2/TiN nanotube heterojunction: nitrogen assisted active hydrogen mechanism. *Chinese J Catal* 2023;47:243-53. DOI

52. Cao Y, Wei Y, Wan W, et al. Photoelectrochemical reduction of CO_2 catalyzed by a 3D core-shell $NiMoO_4$@ZnO heterojunction with bicentre at the (111) plane and thermal electron assistance. *J Mater Chem A* 2023;11:4230-7. DOI

53. Wan W, Zhang Q, Wei Y, et al. p-n heterojunctions of Si@WO_3 mimicking thylakoid for photoelectrocatalytic CO_2 reduction to C_{2+} products - morphology control. *Chem Eng J* 2023;454:140122. DOI

54. Kumaravel V, Bartlett J, Pillai SC. Photoelectrochemical conversion of carbon dioxide (CO_2) into fuels and value-added products. *ACS Energy Lett* 2020;5:486-519. DOI

55. Chu S, Rashid RT, Pan Y, Wang X, Zhang H, Xiao R. The impact of flue gas impurities and concentrations on the photoelectrochemical CO_2 reduction. *J CO2 Util* 2022;60:101993. DOI

56. Jiang X, Chen R, Chen YX, Lu CZ. Proton exchange membrane fuel cells: application for value-added chemical productions. *Chem Synth* 2024;4:6. DOI

57. Gao D, Wei P, Li H, Lin L, Wang G, Bao X. Designing electrolyzers for electrocatalytic CO_2 reduction. *Acta Phys Chim Sin* 2021;37:2009021. DOI

58. Castro S, Albo J, Irabien A. Photoelectrochemical reactors for CO_2 utilization. *ACS Sustainable Chem Eng* 2018;6:15877-94. DOI